RSC Advances

ROYAL SOCIETY OF CHEMISTRY

www.rsc.org/advances

RSC Advances RSCPublishing

ARTICLE

Cite this: DOI: 10.1039/x0xx00000x

Received 00th January 2012,
Accepted 00th January 2012

DOI: 10.1039/x0xx00000x

www.rsc.org/advances

Mo(VI) complex supported on Fe_3O_4 nanoparticles: Magnetically separable nanocatalysts for selective oxidation of sulfides to sulfoxides

Hasan Keypour[#,a], Masomeh Balali[a], Mohammad Mehdi Haghdoost[b], Mojtaba Bagherzadeh[*,b]

A molybdenum complex, $[MoO_2Cl_2(DMSO)_2]$, was immobilized on amino propyl and Schiff base modified magnetic Fe_3O_4@SiO_2nanoparticles by covalent linkage. The resulting nanoparticles were used as efficient and recyclable catalysts for the selective oxidation of sulfides to sulfoxides using urea hydrogen peroxide as the oxidant. The complete characterization of catalysts was carried out by means of thermogravimetric analysis (TGA), scanning electron microscopy (SEM), transmission electron microscopy (TEM), vibrating sample magnetometer (VSM), X-ray photoelectron spectroscopy (XPS), elemental analysis, FT-IR and Raman microprobe techniques.

1. Introduction

Nanomagnetic catalyst is an exponentially growing research field in modern science that exhibits unique properties and application of nanoparticles of different sizes and shapes.[1-3] They have been widely applied to some important reactions such as Suzuki and Heck couplings as well as oxidation of sulfides and thiols.[4-8] Although many catalytic oxidation reactions using homogeneous catalysts have been successfully demonstrated, the difficulties in separating of the catalysts greatly restrict their applications in practice. Heterogeneous catalysts usually need tedious procedures such as filtration and centrifugation for recycling after reactions. This shortcoming could be overcome using magnetic nanoparticle supports because these particles have unique magnetic properties that allow simple separation from the reaction mixture using an external magnet without filtration.[9-10]

Iron oxides particles have been paid growing attention owing to their unique properties and potential applications in various fields, such as magnetic resonance imaging (MRI) contrast agents[11], magnetically assisted drug delivery[12], hyperthermia[13] and recycling of catalysts.[4-6] Magnetite (Fe_3O_4) is generally accepted as being appropriate and safe for in vivo biomedical applications, non-toxic, hydrophilic, and biocompatible, and they have to remain stable in aqueous colloidal suspensions.[14] However magnetic nanoparticles must be stabilized by protective agent against the tendency towards agglomeration.[15] Therefore, the surfaces of Fe_3O_4nanomagnetic were often coated by inert materials such as silica or titanium dioxides to prevent their aggregation and improve their chemical stability.[9,16-18] There are only a limited number of molecules that can be directly bonded to Fe_3O_4 nanoparticles surfaces. On the other hand, after coating, grafting of the metal complexes on the surface of Fe_3O_4 nanoparticles is also possible.[9,15,16]

The Schiff base moiety is one of the preferred functional groups for anchoring different catalytic species on the magnetic nanoparticles.[4,19,20] In this study, new heterogeneous nanocatalysts were synthesized by the covalent anchoring of $[MoO_2Cl_2(DMSO)_2]$ complex on the amino propyl and Schiff base coated magnetic nanoparticles as active, magnetically separable oxidation catalysts. Furthermore, the obtained catalysts showed not only high catalytic activity in oxidation reactions but also high degree of chemical stability in various organic solvents.

2. Results and discussion

As illustrated in Scheme 1, the synthesis of the MNPs is a multistep procedure. First, superparamagnetic Fe_3O_4 (**1**) nanoparticles were prepared by the co-precipitation method.[21] In the next step, the surface of Fe_3O_4 was encapsulated with silica in order to increase the functionality and stability of nanoparticles. For this purpose, the silica-coated MNPs (Fe_3O_4@SiO_2 (**2**)) were synthesized by basic hydrolysis and condensation of TEOS on the surface of the Fe_3O_4nanoparticles.[21]The silica coated Fe_3O_4 nanoparticles were surface-modified with 3-aminopropyltriethoxysilane (APTS) which introduced -NH_2 group on to the surface of support.[22]

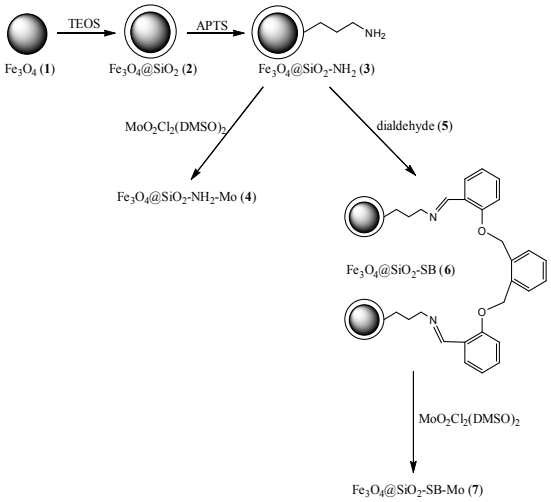

Scheme 1. Step-by-step synthesis of the nanocatalyst.

After functionalization by APTS, free amino groups on the surface of Fe_3O_4@SiO_2-NH_2 nanoparticles can act as monodentate ligands and offer binding sites for immobilization of many metal complexes. With this idea in mind, Fe_3O_4@SiO_2-NH_2-Mo nanoparticle was obtained by the reaction between Fe_3O_4@SiO_2–NH_2 (**3**) and $MoO_2Cl_2(DMSO)_2$ complex. The DMSO ligands in the $MoO_2Cl_2(DMSO)_2$ complex are highly labile toward substitution and can be replaced by the amine group of the surface. It is noteworthy that the release of DMSO was confirmed by GC analysis of reaction mixture. The obtained nanoparticle was characterized by means of FT-IR, EDX, SEM and TGA.

In FT-IR spectrum of APTS-coated Fe_3O_4 NPs (**3**), the absorption bands in 2916 and 2850 cm^{-1} (Fig. 1 (b)) ascribed to C-H stretch of the propyl group .[22] In addition, the presence of magnetite is evident at 610 cm^{-1}. The broad band at 1057 cm^{-1} is the characteristic peak of the Si-O-Si group.[23]

Compared with the FT-IR spectrum of Fe_3O_4@SiO_2-NH_2 (**3**) (Fig. 1 (b)), the characteristic peaks at 922 and 892 cm^{-1} corresponding to the vibration modes of *cis*-MoO_2 moiety can be clearly observed in the FT-IR spectrum of Fe_3O_4@SiO_2-NH_2-Mo (**4**) nanoparticles (Fig. 1 (c)). These absorption bands were also observed in the FT-IR spectrum of starting $MoO_2Cl_2(DMSO)_2$ complex (Fig. 1 (a)) which proves that Mo-dioxo core has successfully bonded to the surface of the Fe_3O_4@SiO_2-NH_2 nanoparticles.[24]

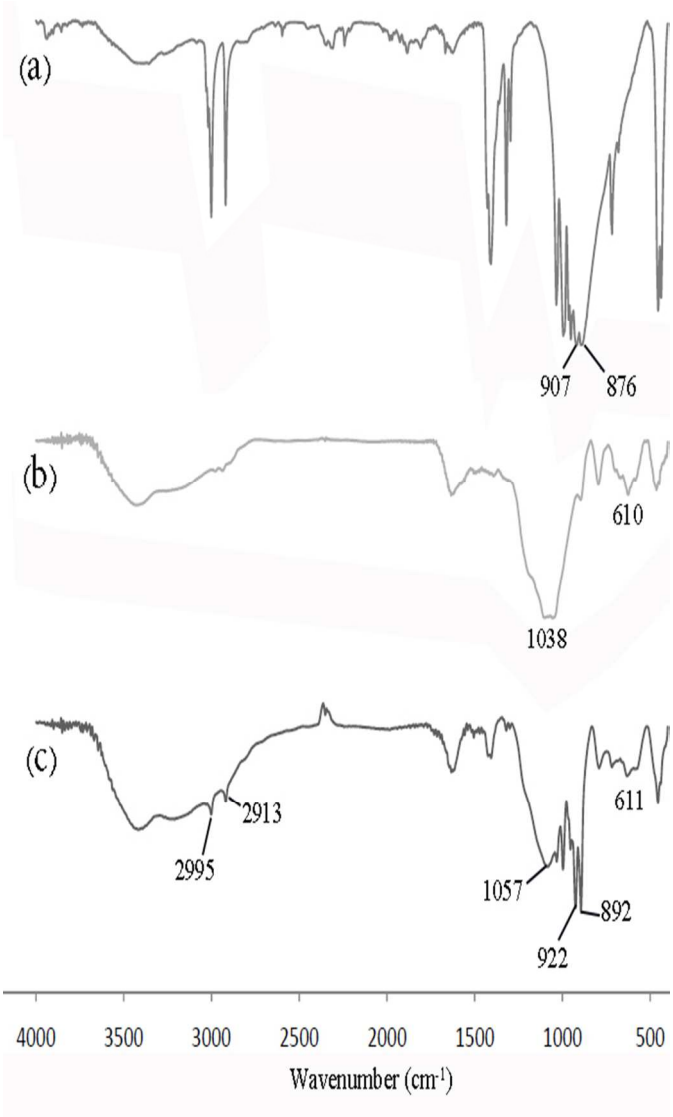

Fig. 1. FT-IR spectra of (a) $MoO_2Cl_2(DMSO)_2$, (b) Fe_3O_4@SiO_2-NH_2, (c) Fe_3O_4@SiO_2-NH_2-Mo.

The chemical identity of the Fe_3O_4@SiO_2 (**2**) and Fe_3O_4@SiO_2-NH_2 (**3**) nanoparticles were confirmed by EDX analysis (Fig. S1 and Fig. S2). EDX analysis of the Fe_3O_4@SiO_2-NH_2-Mo (**4**) nanoparticles (Fig. 2) showed expected elements such as iron, oxygen, silicon, carbon, nitrogen, chlorine and molybdenum. The EDX indicated the presence of Cl within the nanoparticle structure, revealed that the Mo-Cl bonds remain intact during the grafting process. In addition, the molybdenum content of the nanoparticle (**4**) was determined by the inductively coupled plasma optical emission spectroscopy (ICP/OES) analysis to be about 1.6 mmol g^{-1}. This loading value is much higher than that previously reported for similar system[24], suggesting that the immobilization method is very effective.

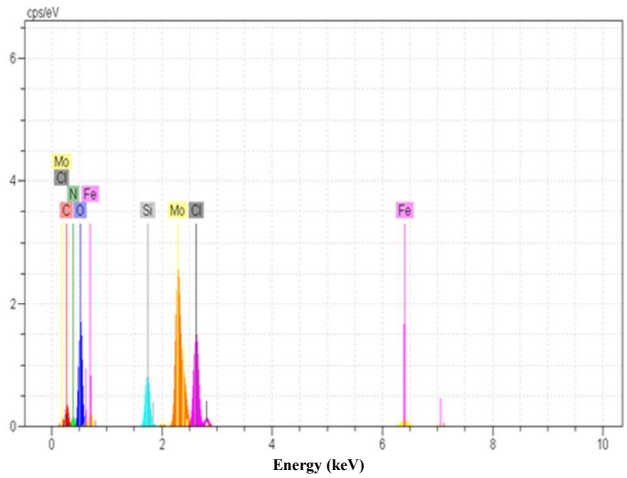

Fig. 2. The energy-dispersive X-ray spectroscopy (EDX) of the Fe_3O_4@SiO_2-NH_2-Mo (**4**).

The particle morphology and textural properties of nanoparticles (**4**) were studied by SEM and representative images are shown respectively in Fig. 3.[25] In the SEM image, nanoparticles with spherical shapes are observed with particle diameter in the range of 70-100 nm.

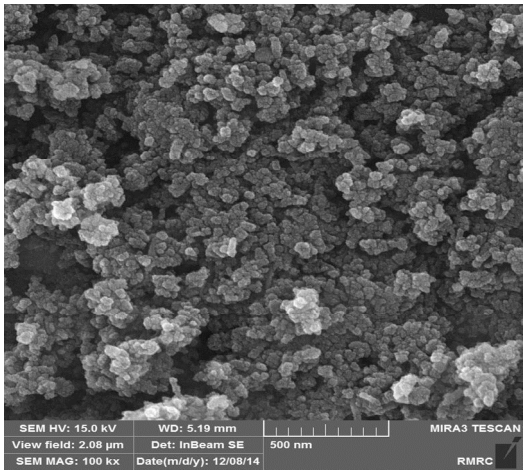

Fig. 3. SEM images of Fe_3O_4@SiO_2-NH_2-Mo(**4**).

The thermogravimetric analysis (TGA) curve of the Fe_3O_4@SiO_2-NH_2-Mo (**4**) shows the multistep mass loss of the organic materials between 50-600 ºC (Fig. 4). Fig. 4 indicates that there exist three distinct weight loss stages during the nanoparticle pyrolysis. According to TGA analysis, the residual mass percent of silica coated NPs is about 54% at 600 ºC. The weight loss of 27% from 50 to 200 ºC is mainly due to the loss of physically adsorbed water, while the second and third weight loss peaks in the range of 200-600 ºC ascribe to the loss of organic amino propyl linkage.[23]

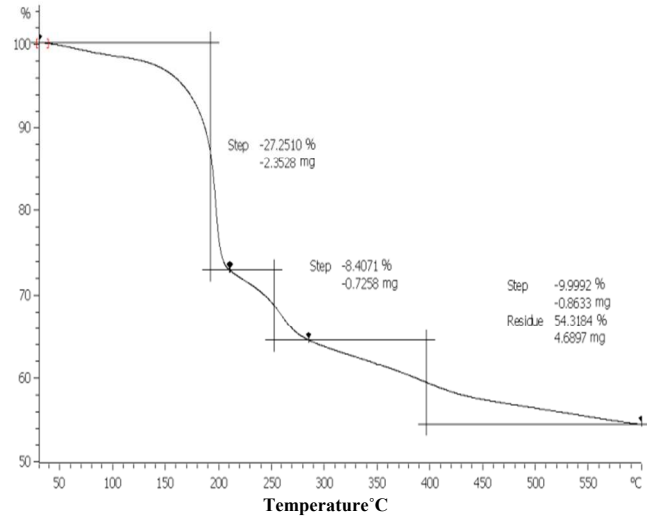

Fig. 4. TGA analysis of Fe_3O_4@SiO_2-NH_2-Mo (**4**).

After functionalization by APTS, free amino groups on the nanoparticle surface can react not only with various transition metal complexes but also with many different carbonyl compounds to form Schiff base ligands. For preparation of Fe_3O_4@SiO_2-SB nanoparticles (**6**), Fe_3O_4@SiO_2-NH_2 (**3**) nanoparticles were reacted with 1,2-bis(2-formylphenoxymethyl)benzenedialdehyde (**5**). Undoubtedly, the Schiff base ligand on the surface of Fe_3O_4@SiO_2-SB nanoparticles has a high ability to form complex with many transition metal centers which makes the Fe_3O_4@SiO_2-SB nanoparticles a suitable candidate for immobilization applications. With respect to this, we made Fe_3O_4@SiO_2-SB (**6**) react with the $MoO_2Cl_2(DMSO)_2$ complex in dry CH_2Cl_2 to synthesize Fe_3O_4@SiO_2-SB-Mo (**7**).

The FT-IR spectrum of the Fe_3O_4@SiO_2-SB-Mo nanoparticle (Fig. 5(c)) clearly showed the formation of molybdenum complex, as exemplified by the appearance of ν(Mo=O) bands in 930 and 886 cm^{-1}. These two bands also exist in the FT-IR spectrum of the unreacted $MoO_2Cl_2(DMSO)_2$ complex (Fig. 5(a)).[24] In addition, the shift of absorption band assigned to the C=N bonds from 1639 in Fe_3O_4@SiO_2-SB to 1664 cm^{-1} in Fe_3O_4@SiO_2-SB-Mo confirmed the coordination of Schiff base ligand.

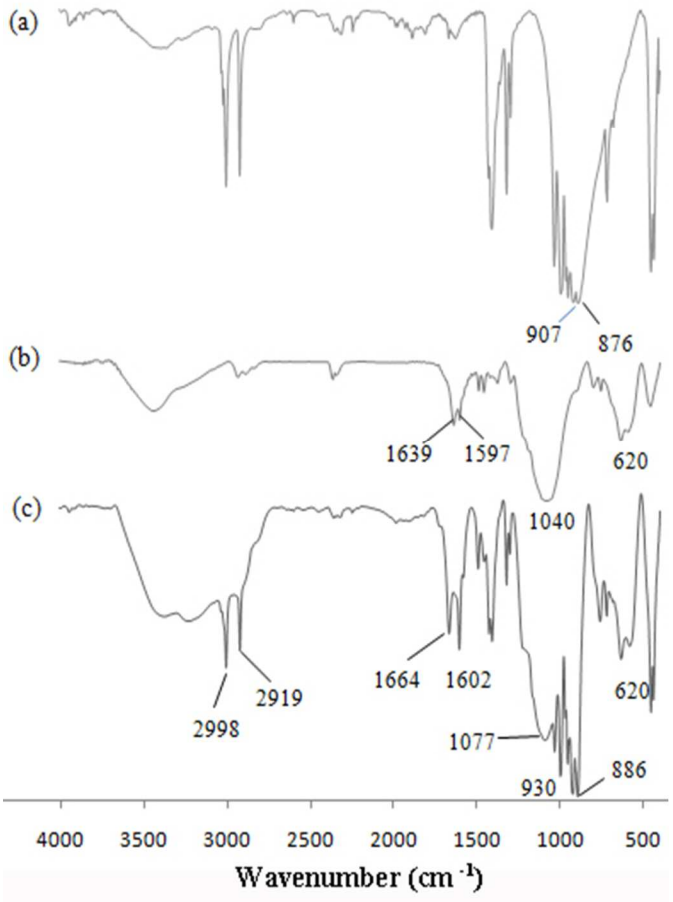

Fig. 5. FT-IR spectra of (a) $MoCl_2O_2(DMSO)_2$ complex, (b) Fe_3O_4@SiO_2-SB and (c) Fe_3O_4@SiO_2-SB-Mo.

Transmission electron microscopy (TEM) and SEM images of nanoparticle (**7**) are shown in Fig. 6 and Fig. 7, respectively. These image revealed that the Fe_3O_4@SiO_2-SB-Mo consist of hundreds of nanometer-sized particles (< 100 nm) as the major component.[26]

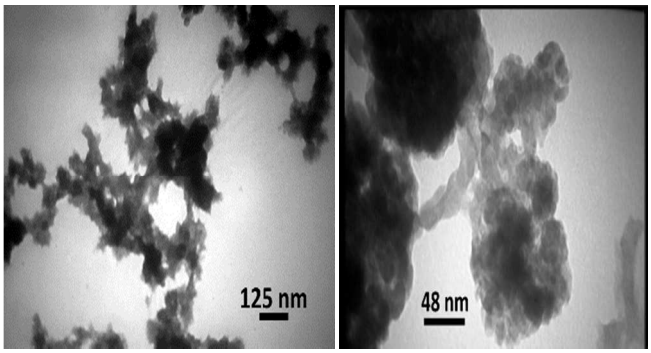

Fig. 6. TEM images of nanoparticle (**7**).

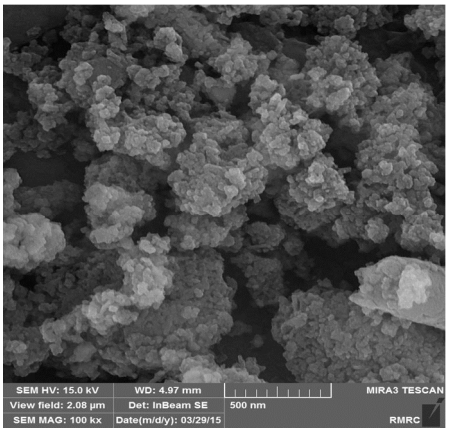

Fig. 7. SEM images of nanoparticle (**7**).

Similar to the TGA curve of nanoparticle **4**, that of Fe_3O_4@SiO_2-SB-Mo (**7**) shows the multistep mass loss of the organic materials as a function of temperature (Fig. 8). The first weight loss of about 37% between 100-220 ºC is due to the removal of physically adsorbed water or solvent.[23] The weight loss of about 6% between 200-300 °C and of about 10% between 300-600 °C may be associated with the thermal degradation of complex and organic groups. According to this TGA analysis, the residual mass percent of nanoparticles is 50% at 600 °C.

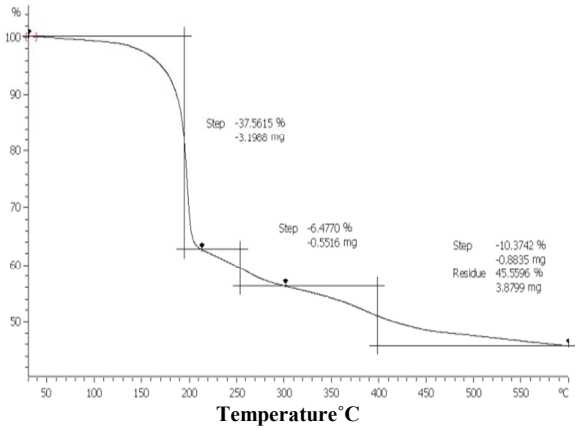

Fig. 8. The TGA curve of Fe_3O_4@SiO_2-SB-Mo (7).

In addition, the EDX survey of the Fe_3O_4@SiO_2-SB-Mo nanoparticles (Fig. 9) confirmed the presence of molybdenum in the nanoparticles structure. The loading amount of molybdenum was about 0.7 mmol g^{-1}, which is determined by ICP/OES analysis. The amount of Mo contain is very similar to that of previously reported study and would normally be sufficient for providing high catalytic activity. [24] The EDX peaks were also observed for all other expected elements such as; iron, oxygen, silicon, carbon, nitrogen and chlorine.

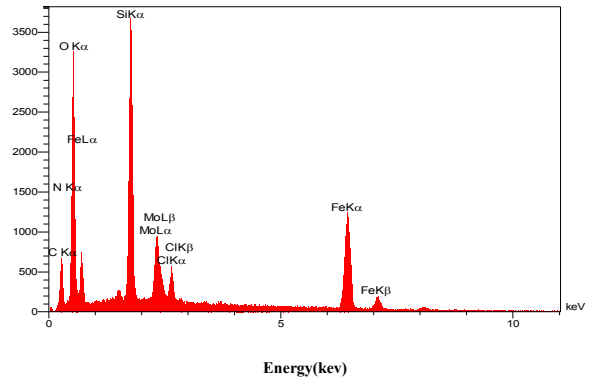

Fig. 9. The EDX analysis of the nanoparticle **7**.

X-ray photoelectron spectroscopy (XPS) was applied to determine the oxidation state of the Mo content (Fig. 10 and Fig S3). The XPS spectrum of Fe_3O_4@SiO_2-SB-Mo nanoparticle revealed two binding energy at 232.70 eV ($3d_{5/2}$) and 235.90 eV ($3d_{3/2}$) which were assigned to Mo(VI) species coordinated to nitrogen or oxygen groups.[27, 28] In addition, the fact that the element of Fe can't be detected in XPS analysis (Fig. S3) confirms the Fe_3O_4 cores are completely coated with silica layer.

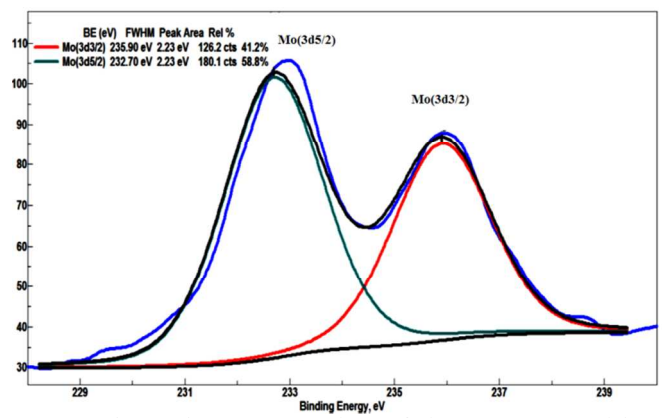

Fig. 10. The Mo3d XPS spectrum of Fe_3O_4@SiO_2-SB-Mo nanoparticle.

The successful immobilization of molybdenum dioxo complex was also confirmed by means of Raman spectroscopy. Fig. 11 shows the Raman spectrum (from 200 to 1000 cm^{-1}) of final Fe_3O_4@SiO_2-SB-Mo nanoparticles. Raman bands at low wavenumbers (224 and 303 cm^{-1}) come from vibrations of Fe-O bonds of Fe_3O_4 core.[29] Beside, the Fe_3O_4@SiO_2-SB-Mo nanoparticles (**7**) possess a Raman band for the stretching mode of the Mo=O bond at around 920 cm^{-1} and 899 cm^{-1}. These two bands can be taken as an unambiguous evidence for successful immobilization of molybdenum complex on the magnetic nanoparticles.[30,31]

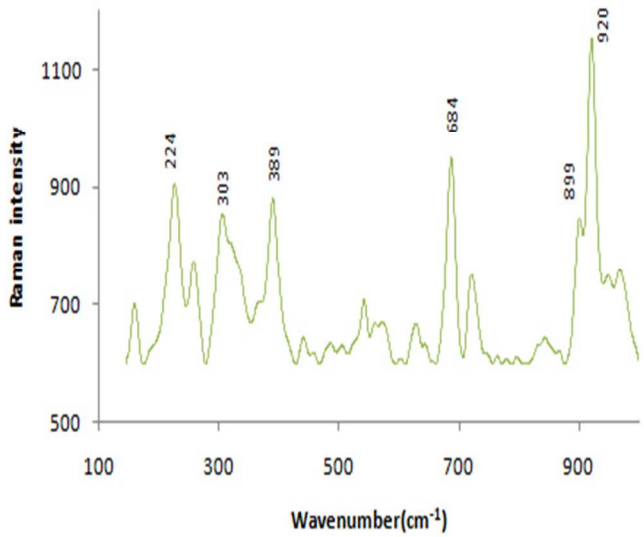

Fig. 11. Raman Microprobe spectrum for of nanoparticle **7.**

Table 1 shows comparative CHN analysis of three nanoparticles: Fe_3O_4@SiO_2-NH_2 (**3**), Fe_3O_4@SiO_2-SB (**6**) and Fe_3O_4@SiO_2-SB-Mo (**7**). According to the CHN analysis, the formation of Schiff base is evident by significant increase in C/N ratio from 3.7 in Fe_3O_4@SiO_2-NH_2 to 29.1 in Fe_3O_4@SiO_2-SB. The C, N and H percentages in Fe_3O_4@SiO_2-SB-Mo (**7**) is lower than two other nanoparticles, mostly due to the molybdenum content.[21]

Table 1. Elemental analysis of Fe_3O_4@SiO_2-NH_2 (**3**), Fe_3O_4@SiO_2-SB (**6**) and Fe_3O_4@SiO_2-SB-Mo (**7**).

Elemental analysis	%C	%N	%H
Fe_3O_4@SiO_2-NH_2	9.73	2.589	2.22
Fe_3O_4@SiO_2-SB	32.18	1.105	3.82
Fe_3O_4@SiO_2-SB-Mo	13.66	0.6419	3.28

Magnetic measurements of the samples were investigated by a vibrating sample magnetometer (VSM) at room temperature (Fig. 12). According to the magnetization curves, the saturation of the nanoparticles decreased from 60 emu/g in the initial Fe_3O_4 sample to 10 emu/g in the final Fe_3O_4@SiO_2-SB-Mo nanoparticle (**7**). This drop in saturation might very well be resultant of the surface coating and surface functionalization of Fe_3O_4 nanoparticles.[24] It is noteworthy that the most significant magnetization decrease occurred in the coating of Fe_3O_4 nanoparticles with silica layer.

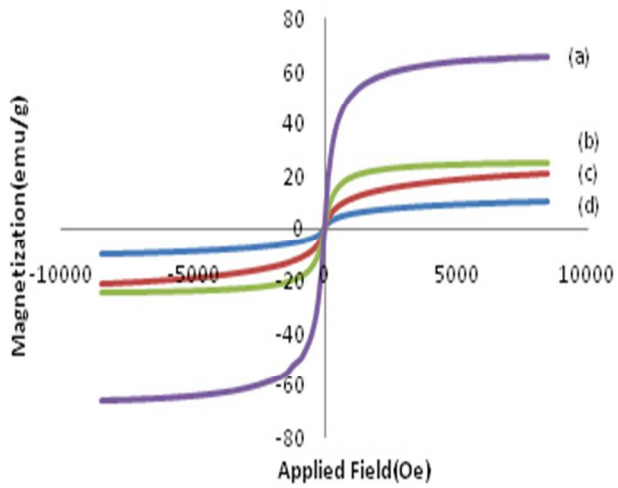

Fig. 12. The VSM analysis of (a) Fe_3O_4, (b) Fe_3O_4@SiO_2, (c) Fe_3O_4@SiO_2-SB and (d) Fe_3O_4@SiO_2-SB-Mo.

The chemoselective oxidation of sulfides to their corresponding sulfoxides is a fundamental chemical reaction because sulfoxides are valuable synthetic intermediates for the synthesis of chemically and biologically significant molecules.[32] Table 2 shows results for nanoparticles **4** and **7** used in the oxidation of sulfides to sulfoxides. In the first cycle, it is thought that the catalytic activity and selectivity of both catalysts are comparable. Using nanocatalysts **4** and **7**, the oxidation of methylphenyl, diethyl, diphenyl and ethylphenyl sulfide resulted in the formation of corresponding sulfoxides in good yields (60-99%) and selectivities (90-100%). Control experiments indicated that no oxidation occurred in the absence of either nanocatalysts or oxidant. In addition, the use of Fe_3O_4@SiO_2 (**2**) or Fe3O4@SiO_2-NH_2 (**3**) nanoparticles in place of nanoparticles **4** and **7** did not promote oxidation.

In the case of dioctyl sulfide, both catalysts mutually showed a reduced activity with respect to the conversion of substrate (Table 2, entries 20 and 21). However, although these two nanocatalysts exhibited high catalytic performance in the first use, each nanocatalyst demonstrated clearly different stability and recyclability results. As summarized in Table 2, the Fe_3O_4@SiO_2-NH_2-Mo nanoparticle (**4**) lost its catalytic activity completely at the second catalytic cycle. In contrary, even after five successive usages, the Fe_3O_4@SiO_2-SB-Mo nanoparticle (**7**) retained its catalytic activity as well as its magnetic property. These results indicate the higher stability of the Schiff base containing Fe_3O_4@SiO_2-SB-Mo compare with the Fe_3O_4@SiO_2-NH_2-Mo nanoparticles. We believe that the formation of Schiff base on the surface of MNPs resulted in the higher chelating ability of ligand and, of course, the higher stability Fe_3O_4@SiO_2-SB-Mo nanoparticles.

In order to evaluate the stability of Fe_3O_4@SiO_2-SB-Mo (**7**) nanocatalyst, after each catalytic reaction, the catalyst particles were collected at the bottom of the test tube using a magnet, supernatant carefully decanted and analyzed by ICP-OES analysis to determine the amount of molybdenum leaching. ICP-OES analysis did not show any leaching of molybdenum species into the solution. In addition, hot filtration test was performed in which the heated solution of Fe_3O_4@SiO_2-SB-Mo nanocatalyst was filtrated while substrate and oxidant were immediately added to the filtrate to initiate the reaction. The hot filtration indicated that some form of soluble molybdenum species were leached from the nanocatalyst and were active for oxidation reaction.

Table 2. Oxidation of sulfides by nanoparticles **4** and **7** in the presence of UHP oxidant.[a]

Ent.	Substrate	Catalyst	Cycle	Conv.[b] (%)	Sel.[c] (%)	TON
1	methylphenyl sulfide	**4**	1	75	90	43
2	methylphenyl sulfide	**4**	2	-	-	-
3	methylphenyl sulfide	**7**	1	86	92	49
4	methylphenyl sulfide	**7**	2	83	95	47
5	methylphenyl sulfide	**7**	3	80	90	46
6	methylphenyl sulfide	**7**	4	81	89	46
7	methylphenyl sulfide	**7**	5	80	89	46
8	diethyl sulfide	**4**	1	75	90	43
9	diethyl sulfide	**4**	2	-	-	-
10	diethyl sulfide	**7**	1	99	100	57
11	diethyl sulfide	**7**	2	99	100	57
12	diethyl sulfide	**7**	3	99	100	57
13	diethyl sulfide	**7**	4	98	100	56
14	diphenyl sulfide	**4**	1	60	100	34
15	diphenyl sulfide	**4**	2	-	-	-
16	diphenyl sulfide	**7**	1	63	100	35
17	diphenyl sulfide	**7**	2	59	100	34
18	ethylphenyl sulfide	**4**	1	85	100	49
19	ethylphenyl sulfide	**7**	1	85	100	49
20	dioctyl sulfide	**4**	1	45	100	26
21	dioctyl sulfide	**7**	1	50	100	28

[a] Reaction condition: sulfide (0.4 mmol), UHP (0.45 mmol), molybdenum nanocatalyst (0.007 mmol), 0.5 mL CH_2Cl_2, 0.5 mL MeOH, room temperature, 30 min.
[b] Determined by GC using chlorobenzene as an internal standard.
[c] Determined by GC, Selectivity to sulfoxide = [sulfoxide %/(sulfoxide % + sulfone %)] × 100.

Base on the previously reported study [33], we postulated a mechanism for the oxidation of sulfides by nanocatalyst **7**. The first step of the mechanism involves the reaction between the molybdenum dioxo complex and UHP oxidant to produce oxo-peroxo compound and water. The nucleophilic attack of the sulfide on one oxygen atom of the peroxo ligand, yielding sulfoxide and regenerating the molybdenum(VI) dioxo complex, which reenters the cycle.

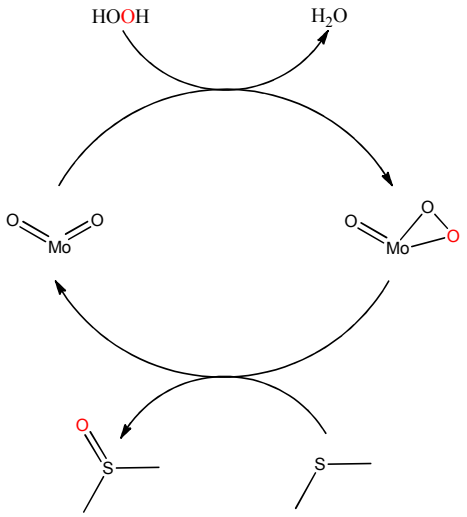

Scheme 2. The postulated mechanism for the oxidation of sulfides by nanocatalyst **7** in the presence of UHP oxidant.

3. Conclusions

In summary, herein we report two methods for the immobilization of molybdenum(VI) complex on silica-coated MNPs. The obtained nanoparticles were characterized with various characterization methods and employed as catalysts for the selective oxidation of sulfides to corresponding sulfoxides using urea-hydrogen peroxide as the oxidant. The catalysts showed the similar catalytic activity but different stability and recyclability. Immobilization of Mo(VI) complex on the MNPs trough the Schiff base ligand resulted in the formation of nanocatalyst that could be recycle more than four times. In contrary, the immobilization through the amino propyl linkage did not lead to the formation of a highly stable and fully recyclable nanocatalyst.

4. Experimental section

4.1. Materials

Tetraethoxysilane (TEOS), 3-aminopropyltriethoxysilane (APTS), 2-hydroxybenzaldehyde, 1,2-bis(bromomethyl)benzene were purchased from Aldrich. All commercially available solvents and tested compounds were of analytical-reagent grade and used without further purification.

4.2. Characterization methods

Gas chromatographic (GC) analyses were performed on an Agilent Technology 6890N, 19019J-413 HP-5, 5% phenyl methyl siloxane, capillary 60m×250mm×1mm. Elemental analyses (C, H, and N) were performed using a Heraeus Elemental Analyzer CHN-O-Rapid (Elementar-Analysesystem, GmbH). IR spectra were recorded as KBr pellets using a Perkin Elmer Spectrum Version 10.01.00 spectrophotometer. Measures of pH were carried out by a Mettler Toledo S40 Seven MultiTM pH-meter. Raman spectrum was measured by Confocal depth profiling with True Focus BRUKER (Germany) equipped with high-energy laser diodes. Scanning electron microscopy (SEM) was carried out on Philips XL30. The TGA/DTA curves were determined using 851 Mettler Toledo apparatus. The heating rate was 5 K/min. X-ray photoelectron spectroscopy (XPS) was carried out by Dual anode (Mg and Al Kα) a chromatic X-ray source. Magnetic measurement of materials was investigated with a vibrating sample magnetometer VSM (4 inch, Daghigh Meghnatis Kashan Co., Kashan, Iran) at room temperature. Transmission electron microscopy (TEM) images were obtained on an EM10C (Zeiss) transmission electron microscope at an accelerating voltage of 80 kV. Samples dispersed in solution were cast onto a carbon-coated copper grid.

4.2. Preparation of MNPs(Fe_3O_4@SiO_2-NH_2) (3)

Fe_3O_4 (**1**) and Fe_3O_4@SiO_2 (**2**) magnetic nanoparticles were prepared according to the reported method.[21]The obtained Fe_3O_4@SiO_2 nanoparticles were dried under vacuum and then modified with 3-aminopropyltriethoxysilane (APTS).[22]

4.3. Synthesis of Fe_3O_4@SiO_2-NH_2-Mo nanocatalyst (4)

1 g of Fe_3O_4@SiO_2-NH_2 (**3**) was suspended in CH_2Cl_2 (50 mL). Then, $MoO_2Cl_2(DMSO)_2$ (0.7 mmol) in 15 mL CH_2Cl_2 was added and the mixture was stirred for 24 h under a nitrogen atmosphere. After separation with an external magnet, the product was washed with CH_2Cl_2 to remove unreacted molybdenum precursor**.**

4.4. Synthesis of 1,2-bis(2-formylphenoxymethyl)benzene (5)

Sodium salt of 2-hydroxybenzaldehyde was prepared by adding solution of NaOH (6.25 mmol in 20mL water) to a solution of salicaldehyde (6.25 mmol) in 25 mL of ethanol and stirring at 60 ºC for 30 min. To this, a solution of 1,2-bis(bromomethyl)benzene (0.822 g, 3.125 mmol) in EtOH (20 mL) was added and refluxed For 24 h. The solution was cooled and the solid product was filtered off and recrystallized from acetonitrile.[34] Yield: 0.629 g (58%). m.p. 114 °C; ^{1}HNMR (90 MHz, $CDCl_3$): 5.26 ppm (s, 4H, CH_2), 7.05-7.98 ppm (m, 12H, ArH), 10.41ppm (s, 2H, CHO); ^{13}CNMR (90 MHz, $CDCl_3$): 188.5, 160, 135.5, 133.9, 128.8, 128.5, 124, 120, 112, 68 ppm.

4.5. Synthesis of Fe_3O_4@SiO_2-SB (6)

Fe_3O_4@SiO_2-NH_2 (**3**) was suspended in 100 mL of methanol with sonication. 1,2-bis(2-formylphenoxymethyl)benzene (**5**) (0.8 mmol) was added to this mixture and the resulted mixture was refluxed for 24 h. The resultant solid was separated magnetically and then washed with methanol several times to remove the unreacted residue of the dialdehyde and dried under vacuum at 303 K.

4.6. Synthesis of Fe_3O_4@SiO_2-SB-Mo nanocatalyst (7)

For the preparation of Mo(VI) nanocatalyst, $MoO_2Cl_2(DMSO)_2$ (1 mmol) was dissolved in CH_2Cl_2 (50 mL). 1 g of Fe_3O_4@SiO_2-SB (**6**)

was then added to this solution and stirred for 24 h under a nitrogen atmosphere. After separation with an external magnet, the product was washed with CH_2Cl_2 to remove unreacted molybdenum precursor.

4.7. General conditions for catalytic oxidation of sulfides

A typical reaction using the Mo(VI) nanocatalyst and sulfides is described as follows: Chlorobenzene (40 mL, 0.4 mmol) as the internal standard and nanocatalyst **7** (0.01 g, 0.007 mmol of molybdenum complex) were added to a solution of sulfide (0.4 mmol) in (1:1) a mixture of CH_3OH-CH_2Cl_2 (1 mL), then UHP (0.042 g, 0.45 mmol) as the oxidant was added to the resulting mixture and stirred at room temperature for 30 min. The nanocatalyst was separated using a magnetic field and the formation of products was monitored by GC. To clearly carry out the identity of the products, the retention times and spectral data of the products were compared with those of commercially available sulfoxides and sulfones. At the end of reaction, the catalyst particles were washed with methanol and DCM for several times, were dried in vacuum and could be reused.[22]

Acknowledgements

We are grateful to the Faculty of Chemistry of Bu-Ali Sina University for financial support. We also acknowledge the Research Council of Sharif University of Technology for research funding of this project.

Notes

[a]Chemistry Department, Bu-Ali Sina University, Hamedan Department of Chemistry, Bu-Ali Sina University, Hamadan. E-mail:haskey1@yahoo.com

[b]Chemistry Department, Sharif University of Technology, Tehran, Iran. Email:bagherzadeh@sharif.edu

References

1 F.Matloubi-Moghaddam and S.E.Ayati, *RSC Adv.,* 2015, **5**, 3894-3902.
2.J. Safari and L. Javadian, *RSC Adv.*, 2014,**4**, 48973-48979.
3.N.Zohreh, S.H. Hosseini, A. Pourjavadi and C. Bennett, *RSC Adv.*, 2014, **4**, 50047-50055.
4. H. Wang, Y. Zhang, H. Yang, Z. Ma, F. Zhang, J. Sun and J. Ma, *Microporous Mesoporous Mater*., 2013, **168**, 65-72.
5. S. Lia, W. Zhanga, M. Sob, C. Cheb, R. Wanga and R. Chena, *J. Mol. Catal. A: Chem*. 2012, **359**, 81-87.
6. N.J.S. Costa, P.K. Kiyohara, A.L. Monteiro, Y. Coppel, K. Philippot and L.M. Rossi, *J. Catal*., 2010, **276**, 382-389.
7.A. Rostami and B. Atashkar, *J. Mol. Catal. A: Chem.*, 2015, **398,** 170-176.
8. E. Karaoglu, A. Baykal, M. Senel, H. Sozeri and M.S. Toprak, *Mater. Res. Bull.*, 2012, **47**, 2480-2486.
9. C.W. Lim and I.S. Lee, *Nano Today*, 2010, **5**, 412-434.
10. Y.C. Chang and D.H. Chen, *J. Hazard. Mater*., 2009, **165**, 664-669.
11. C. Sanjaia, S. Kothana, P. Gonilb, S. Saesoob and W. Sajomsang, *Carbohydr. Polym.*, 2014, **104**, 231-237.
12. J.M. Montenegro, V. Grazu, A. Sukhanova, S. Agarwal, J.M. Fuente, I. Nabiev, A. Greiner and W.J. Parak*, Adv. Drug Deliv. Rev*., 2013, **65**, 677-688.
13. Q.L. Jiang, S.W. Zheng, R.Y. Hong, S.M. Deng, L. Guo, R.L. Hu, B. Gao, M. Huang, L.F. Cheng, G.H. Liu and Y.Q. Wang, *Appl. Surf. Sci.*, 2014, **307**, 224-233.
14. J. Si and H. Yang, *Mater. Chem. Phys*., 2011, **128**, 519-524.
15. M. Khosroshahi and L. Ghazanfari, *Mater. Sci. Eng. C*, 2012, **32,** 1043-1049.
16. S. Campelj, D. Makovec and M. Drofenik, *J. Magn. Magn. Mater.*, 2009, **321**, 1346-1350.
17. X. Peng, Y. Wang, X. Tang and W. Liu, *Dyes Pigm.,* 2011, **91,** 26-32.
18. L. Wang, Y. Sun, J. Wang, J. Wang, A. Yu, H. Zhang and D. Song, *Colloids Surf. B,* 2011, **84**, 484-490.
19. M. Masteri-Farahani and Z. Kashef, *J. Magn. Magn. Mater*., 2012, **324**, 1431-1434.
20. M. Esmaeilpour, A.R. Sardariana and J. Javidi. *Appl. Catal., A*, 2012, **445**, 359-367.
21. M. Bagherzadeh, M.M. Haghdoost and A. Shahbazirad, *J. Coord. Chem*., 2012, **65,** 591-601.
22. M. Bagherzadeh, M.M. Haghdoost, F. Matlobi-Moghaddam, B. Koushki-Foroushani, S. Sarazdi and E. Payab, *J. Coord. Chem*., 2013, **66**, 3025-2036.
23. M.Z. Kassaee, H. Masrouri and F. Movahedi, *Appl. Catal. A*, 2011, **395**, 28-33.
24. M. Masteri-Farahani and N. Tayyebi. *J. Mol. Catal. A: Chem.*, 2011, **348**, 83-87.
25. C.I. Fernandes, M.D. Carvalho, L.P. Ferreira, C.D. Nunes and P.D. Vaz, *J. Organomet. Chem.*, 2014, **760**, 2-10.
26. S. Shylesh, J. Schweizer, S. Demeshko, V. Sch-nemann, S. Ernst and W.R. Thiel, *Adv. Synth. Catal.*, 2009, **351**, 1789-1795.
27. Z. Li, C. Chen, E. Zhan, N. Ta, Y. Li and W. Shen*, Chem. Commun*., 2014, **50,** 4469-4471.
28. L. Barrui, J.M. Campos-Martín, M.P. de Frutos and J.L.G. Fierro, Ind. Eng. Chem. Res. 2008, **47**, 8016-8024
29. C. Guo, Y. Hu, H. Qian, J. Ning and S. Xu, *Mater. Charact*., 2011, **62**, 148 .
30. Q. Tang, Z. Shan, L. Wang and X. Qin, *Electrochim. Acta,* 2012, **79**, 148-153.
31. I.D. Dobrea , C.E. Ciocan, E. Dumitriu, M.I. Popa, E. Petit and V. Hulea, *Appl. Clay Sci*., 2015, **104**, 205-210.
32. H. Zhang and G. Wang, *Tetrahedron Lett*., 2014, **55**, 56-58.
33. M. Amini, M.M. Haghdoost and M. Bagherzadeh, *Coord. Chem. Rev*., 2013, **257,** 1093-1121.
34. H. Keypour, M. Rezaeivala and A.A. Dehghani-Firouzabadi, *J. Chem. Res.*, 2009, 126-128.

